



ALMA MATER STUDIORUM  
UNIVERSITÀ DI BOLOGNA

ARCHIVIO ISTITUZIONALE  
DELLA RICERCA

## Alma Mater Studiorum Università di Bologna Archivio istituzionale della ricerca

Immunohistochemical Analysis of Olfactory Sensory Neuron Populations in the Developing Olfactory Organ of the Guppy, *Poecilia reticulata* (Cyprinodontiformes, Poeciliidae)

This is the final peer-reviewed author's accepted manuscript (postprint) of the following publication:

*Published Version:*

Bettini, S., Lazzari, M., Milani, L., Maurizii, M.G., Franceschini, V. (2023). Immunohistochemical Analysis of Olfactory Sensory Neuron Populations in the Developing Olfactory Organ of the Guppy, *Poecilia reticulata* (Cyprinodontiformes, Poeciliidae). *MICROSCOPY AND MICROANALYSIS*, 29(5), 1764-1773 [10.1093/micmic/ozad099].

*Availability:*

This version is available at: <https://hdl.handle.net/11585/947098> since: 2024-05-20

*Published:*

DOI: <http://doi.org/10.1093/micmic/ozad099>

*Terms of use:*

Some rights reserved. The terms and conditions for the reuse of this version of the manuscript are specified in the publishing policy. For all terms of use and more information see the publisher's website.

This item was downloaded from IRIS Università di Bologna (<https://cris.unibo.it/>).  
When citing, please refer to the published version.

(Article begins on next page)

This is the final peer-reviewed accepted manuscript of:

**Simone Bettini, Maurizio Lazzari, Liliana Milani, Maria Gabriella Maurizii, Valeria Franceschini, Immunohistochemical Analysis of Olfactory Sensory Neuron Populations in the Developing Olfactory Organ of the Guppy, *Poecilia reticulata* (Cyprinodontiformes, Poeciliidae), *Microscopy and Microanalysis*, Volume 29, Issue 5, October 2023, Pages 1764–1773**

The final published version is available online at:  
<https://doi.org/10.1093/micmic/ozad099>

Terms of use:

Some rights reserved. The terms and conditions for the reuse of this version of the manuscript are specified in the publishing policy. For all terms of use and more information see the publisher's website.

*This item was downloaded from IRIS Università di Bologna (<https://cris.unibo.it/>)*

***When citing, please refer to the published version.***

1  
2  
3  
4  
5  
6  
7  
8  
9  
10  
11  
12  
13  
14  
15  
16  
17  
18  
19  
20  
21  
22  
23  
24

**Immunohistochemical analysis of olfactory sensory neuron populations in the developing olfactory organ of the guppy, *Poecilia reticulata* (Cyprinodontiformes, Poeciliidae)**

Simone Bettini<sup>1</sup>†, Maurizio Lazzari<sup>1\*</sup>†, Liliana Milani<sup>1</sup>, Maria Gabriella Maurizii<sup>1</sup>, Valeria Franceschini<sup>1</sup>

<sup>1</sup> Department of Biological, Geological and Environmental Sciences, University of Bologna, Via Selmi 3, 40126 Bologna, Italy

**Olfactory sensory neuron populations in the guppy**

Conflicts of interest: The authors declare none

---

\* Author for correspondence:  
Maurizio Lazzari, Department of Biological, Geological and Environmental Sciences, University of Bologna, Bologna 40126, Italy  
E-mail: maurizio.lazzari@unibo.it  
Phone number: +39 051 2094145

† The first two authors contributed equally to this work.

25 **Abstract**

26 Olfaction is fundamental for sensing environmental chemicals and has obvious adaptive  
27 advantages. In fish, the peripheral olfactory organ is composed of lamellae in which the  
28 olfactory mucosa contains three main categories of olfactory sensory neurons (OSNs): ciliated  
29 (cOSNs), microvillous (mOSNs), and crypt cells. We studied the appearance of these different  
30 OSNs during development of *Poecilia reticulata*, given its growing use as animal model  
31 system. We performed immunohistochemical detection of molecular markers specific for the  
32 different OSNs, carrying out image analyses for marked-cell counting and measuring optical  
33 density. *P. reticulata* olfactory organ did not show change in size during the first weeks of life.  
34 The proliferative activity increased at the onset of secondary sexual characters, remaining high  
35 until sexual maturity. Then it decreased in both sexes, but with a recovery in females, probably  
36 in relation to their almost double body growth, compared to males. The density of both cOSNs  
37 and mOSNs remained constant throughout development, probably due to conserved functions  
38 already active in the fry, independently of the sex. The density of calretinin-positive crypt cells  
39 decreased progressively until sexual maturity, whereas the increased density of calretinin-  
40 negative crypt cell fraction, prevailing in later developmental stages, indicated their probable  
41 involvement in reproductive activities.

42

43 **Keywords:** olfactory epithelium, olfactory sensory neurons, crypt cells, calretinin;  $G_{\alpha \text{ olf}}$ ,  
44 PCNA, guppy, immunohistochemistry, image analysis

45

46

## 47 **Introduction**

48 Olfaction is a phylogenetically ancient sense that has a very important role in animal life, being  
49 fundamentally related to food research and reproductive behavior (Zeiske et al., 1992).

50 Vertebrates develop an olfactory system that detects odorants and pheromones through their  
51 interaction with specialized cell surface receptors on olfactory sensory neurons (OSNs).

52 Olfaction is a form of chemosensation and sensing environmental chemicals has obvious  
53 adaptive advantages, thus it is not surprising that a diversity of chemosensory systems has  
54 evolved in animals (Poncelet & Shimeld, 2020).

55 The main types of fish olfactory sensory neurons (OSNs), common to all other vertebrates, are  
56 bipolar neurons with dendritic processes that reach the surface of the olfactory epithelium,  
57 where they originate olfactory terminal knobs bearing apical differentiations: cilia in ciliated  
58 OSNs (cOSNs) and microvilli in microvillous OSNs (mOSNs) (Riddle & Oakley, 1991; Hansen  
59 & Zeiske, 1998; Farbman, 2000). Ciliated olfactory sensory neurons (cOSNs) and microvillous  
60 olfactory sensory neurons (mOSNs) also differ in location of their cell bodies and length of  
61 their dendrites (Morita & Finger, 1998; Hamdani & Døving, 2007). Ciliated OSNs and mOSNs  
62 have sensitivities to partially overlapping odorant categories, but project into distinct regions  
63 of the olfactory bulb, related to different functions (Hansen et al., 2003; Hamdani & Døving,  
64 2007; Braubach et al., 2012; Bazaes et al., 2013). Other than OSNs, the olfactory epithelium  
65 contains other cell types, such as sustentacular cells and basal stem cells.

66 Fish, in addition to the previously described OSN, also possess a third ovoid-shaped OSN type,  
67 the crypt cell (actinopterygian fish, Hansen et al., 1997; Hansen & Finger, 2000; cartilaginous  
68 fish, Ferrando et al., 2006, 2007). Crypt cells are located in the upper third of the olfactory  
69 epithelium and their apical pole facing the nasal cavity carries both cilia and microvilli. Their  
70 axonal projection patterns in the glomerular layer of the olfactory bulb are uneven among

71 species: in *Ictalurus punctatus* and *Carassius Carassius* crypt neuron terminals are localized to  
72 the ventral region, suggesting a possible association with pheromone perception and  
73 reproductive behavior (Hansen et al. 2003; Weltzien et al., 2003; Hamdani & Døving, 2006).  
74 On the other hand, in *Danio rerio*, crypt cells seem to project to one (Ahuja et al., 2013) or two  
75 (Braubach et al., 2012; Gayoso et al., 2012) dorsomedial glomeruli supposed to be connected  
76 with the medial olfactory tract, that is assumed to convey pheromone detection as well as alarm  
77 response (Ahuja et al., 2013). It is also controversial which odorants crypt cells respond to  
78 (Hamdani & Døving, 2006; Schmachtenberg, 2006; Hamdani et al., 2008; Vielma et al., 2008),  
79 so their function remains unclear. Other two OSN subtypes have been described: kappe cells  
80 and pear-shaped neurons (Ahuja et al., 2014; Wakisaka et al., 2017), but they have not currently  
81 been described in fish other than zebrafish and it is not sure if they can actually be defined as  
82 separate OSN types.

83 The peripheral olfactory organ of fish has a great variability in size, shape and organization in  
84 olfactory lamellae (Yamamoto, 1982; Hansen & Zielinski, 2005). With regard to the structure  
85 of the peripheral olfactory organ, fish can be distinguished into macrosmatic and macrosmatic  
86 species (Lazzari et al., 2013). *Poecilia reticulata*, for example, possesses a small olfactory  
87 cavity containing a single olfactory lamella, therefore it is considered a typical representative  
88 of macrosmatic fish (Lazzari et al., 2007).

89 Fish OSNs are directly exposed to environmental water and any substances it contains, toxicants  
90 included. Alterations in olfaction can affect fish behavior and survival with possible ecological  
91 and socio-economic consequences. *P. reticulata* has become an important model organism for  
92 developmental, ecological and toxicological studies (Kinnberg & Toft., 2003; Bettini et al.,  
93 2006; Antunes et al., 2017; Souza Trigueiro et al., 2021; Milani et al., 2022), and the acquisition  
94 of new information on the development and organization of the olfactory epithelium in this fish  
95 will allow us to extend and strengthen its use as model (Bettini et al., 2012, 2016, 2017).

96 Previously in our laboratory, we analyzed in adult *P. reticulata* both the histological and  
97 ultrastructural organizations of the peripheral olfactory organ (Lazzari et al., 2007), and the  
98 distribution of some molecular markers in the olfactory epithelium (Bettini et al., 2009).  
99 Particular attention was paid to crypt cells whose antigenic response in adults distinguished two  
100 subpopulations, supporting the possibility that crypt cells are functionally less uniform as  
101 supposed (Bettini et al., 2017). Our studies on the development of OSN populations in *P.*  
102 *reticulata* have been so far limited to a subpopulation of crypt cells ~~crypt cell subpopulation~~  
103 (Bettini et al., 2012). The aim of this work is to study the dynamics of the populations of cOSNs,  
104 mOSNs, and a subpopulation of previously unexamined crypt cells, from fish birth to  
105 adulthood.  
106

107 **Materials and Methods**

108 *Animal care and breeding*

109 Adult (older than 6months) *P. reticulata* (Peters, 1859) of both sexes were purchased locally  
110 from Coral Aquarium, Bologna, Italy, acclimated in laboratory conditions using separate  
111 aquaria for each sex containing a 1:2 mixture of dechlorinated tap water and distilled water at  
112 27 °C in a 12/12 h light/dark cycle, and fed twice daily with commercial flake food. After 10  
113 days, females were allowed to mate with males, at a ratio of 3:1 to reduce stressful conditions.  
114 In the following weeks, aquaria were daily monitored for pregnant females, that were isolated  
115 in tanks at the same conditions of aquaria and let give birth. All procedures conformed to the  
116 guidelines of European Communities Council Directive (86/609/CEE), the current Italian  
117 legislation regarding the use and care of animals, and the guidelines issued by the US National  
118 Institutes of Health. The Ethic-Scientific Committee of the University of Bologna also approved  
119 this study (protocol no. 17/79/2014).

120 *Fry collection and tissue sampling*

121 Newborn individuals were isolated immediately after birth in 5 L tanks and sacrificed at  
122 established time points (7, 14, 21, 45 and 90 days safter hatching). We included in the  
123 experiment also adult guppies (about 6-month-old). Fish were previously anesthetized with  
124 0.1% 3-aminobenzoic acid ethyl ester (MS-222, Sigma Chemical, St. Louis, MO, USA) and  
125 immersion fixed in a modified Bouin's solution (saturated aqueous solution of picric acid and  
126 formalin at a ratio of 3:1) for 24 h. Heads from adult guppies were analogously collected and  
127 processed, after removal of dorsal cranial vault to facilitate fixation. All samples were washed  
128 several times in 0.1 M sodium phosphate buffer, pH 7.4, and decalcified in 10%  
129 ethylenediaminetetraacetic acid (EDTA, Fluka, Buchs, SG, CH) in the same buffer for 1-7 days,  
130 depending on specimen age and mineralization. Specimens were finally embedded in Paraplast  
131 plus (Sherwood Medical, St. Louis, MO, USA; melting point 55–57°C), frontally sectioned (5



132  $\mu\text{m}$ ) with Leica 2145 microtome (Leica Microsystems, Milan, IT) and mounted on silanized  
133 slides, two sections/slide. Sections of gonads were stained with Hematoxylin and Eosin to  
134 determine sex of guppy fry and sexual development.

### 135 ***Immunohistochemistry***

136 Serial sections were selected for immunohistochemistry. Following stereological methods,  
137 every 10<sup>th</sup> pair of sections a disector was sampled (Bettini et al., 2009, 2012). Slides from 10  
138 fish (5 males and 5 females) for each time point were processed. Sections were deparaffinized,  
139 rehydrated and immersed in 1% H<sub>2</sub>O<sub>2</sub> (Sigma Chemical, St Louis, MO, USA) for 20 min at RT  
140 to quench endogenous peroxidase. Then antigen retrieval was performed with microwave  
141 treatment at 750 W for 10 min in citrate buffer at pH 6.0. Non-specific binding was blocked  
142 with 10% normal goat serum (NGS; Vector Laboratories, Burlingame, CA, USA) and 1%  
143 bovine serum agglutinin (BSA; Sigma Chemical, ~~St Louis, MO, USA~~), before incubation in  
144 primary antibodies overnight at 4 °C. Then sections were washed and further incubated in  
145 horseradish peroxidase (HRP)-conjugated goat anti-rabbit IgG (1:100; Vector Laboratories) for  
146 polyclonal primary antibodies and goat anti-mouse IgG (1:100; A4416; Sigma) for monoclonal  
147 primary antibody. Finally, the immunoreaction was visualized with 0.1% 3,3-diaminobenzidine  
148 substrate (DAB; Sigma Chemical). Sections from zebrafish olfactory organ were chosen for  
149 positive controls. Negative controls were obtained by replacing the primary antibody with 10%  
150 NGS.

### 151 ***Antibodies***

152 Primary antibodies used were: 1) polyclonal rabbit anti-calretinin (AB5054 [developed against  
153 rat calretinin], Chemicon International, Temecula, CA, USA, 1:1000), a marker for mOSNs  
154 (Bettini et al., 2009) and a subpopulation of crypt cells (Bettini et al., 2017); 2) polyclonal rabbit  
155 anti-G $\alpha_{\text{olf}}$  (sc-383; Santa Cruz Biotechnology, Santa Cruz, CA, USA, 1:500), a marker for  
156 cOSNs (Gayoso et al., 2011; Braubach et al., 2012; Bettini et al., 2016; Lazzari et al., 2017,

157 2019); 3) monoclonal mouse anti-proliferating cell nuclear antigen (anti-PCNA; Clone PC10;  
158 P 8825; Sigma; 1:500) to detect dividing cells (Bettini et al., 2016; Lazzari et al., 2017). All  
159 antibodies were already validated in previous literature: anti-calretinin in guppy (Bettini et al.,  
160 2017); anti-G<sub>α olf</sub>, which recognizes a 42-45 kDa protein under similar experimental conditions,  
161 in zebrafish (Gayoso et al., 2011; Braubach et al., 2012), in catfish (Hansen et al., 2003), in  
162 lamprey (Frontini et al., 2003), and in goldfish (Hansen et al., 2004).

### 163 *Image acquisition and statistical analysis*

164 Micrographs were taken using a BEL BlackL 5000 digital camera (BEL Engineering, Monza,  
165 Italy) mounted on an Olympus BH-2 microscope (Olympus Italia, Segrate, Italy).

166 Figures were assembled with Adobe Photoshop (CS3; Adobe Systems, San Jose, CA, USA),  
167 without content alteration.

168 We used the image analysis software ImageJ (version 1.53t) with Cell Counter plug-in (v.2) to  
169 count calretinin-positive crypt cells and PCNA-positive mitotic cells, and calculate epithelial  
170 volume and cell density (see Bettini et al., 2012 for more details). Immunostaining patterns of  
171 anti-G<sub>α olf</sub> (cOSNs) and anti-calretinin (mOSNs) did not permit cell discrimination and counting  
172 (Bettini et al., 2016; Lazzari et al., 2017, 2019, 2021). Therefore, we considered the optical  
173 density (OD), since the immunostaining intensity can be regarded as an indirect index of the  
174 number of immunopositive cells (Iqbal & Byrd-Jacobs, 2010). In the olfactory epithelium,  
175 ImageJ analysis provided average gray values of immunostained regions and background-  
176 unstained zones. The OD was then calculated as the logarithm of the ratio between gray values  
177 of background and stained Region Of Interest (we excluded the lamina propria and exclusively  
178 selected the area of the epithelium, from the apical margin to the basal membrane). Using Excel  
179 2019 (Microsoft Corporation, Redmond, WA, USA), data are reported in the histograms as  
180 means ± s.e.m. and statistically compared using one-way ANOVA (with LSD (Fisher Least

181 Significant Difference) *post hoc* test) for age groups, and Student's *t*-test for differences  
182 between sexes in each group.

183

184 **Results**

185 In the first 3 time points considered (from 7 to 21 days of age), guppies were in the fry stage;  
186 in the 4<sup>th</sup> time point, at 45 days after birth, they were in the juvenile stage, when gonads reached  
187 their final structure, spermatogenesis started and oogenesis proceeded, secondary sexual  
188 characteristics developed and sexual dimorphism began to manifest; in the 5<sup>th</sup> time point, at 90  
189 days of life fish were in the young stage and they were sexually active, even if sexual maturation  
190 was not complete: in females the eggs were not fully matured, while the males, despite having  
191 begun to court the females, were not yet capable to produce sperm and fertilize eggs. In the next  
192 three months they reached adult stage with fully developed gametes in both sexes (Fig. 1). At  
193 this point, fish size growth stopped or slowed down significantly. For more details see Evans  
194 et al. (2002) and Koya et al. (2003).

195 The olfactory organ of *Poecilia reticulata* contains only one olfactory lamella (Fig. 1a) whose  
196 surface is covered by the sensory epithelium (Fig. 1b). PCNA immunohistochemistry allowed  
197 to evaluate the course of cell proliferation during the considered periods. PCNA-positive cells  
198 were usually located in the basal region of the olfactory lamella (Figs. 2a1, 2b1, 2d1, 2a2, 2b2,  
199 2d2). At stages of 7 and 14 days, the immunohistochemical staining was very reduced with very  
200 few positive cells detected in the lamellae of both sexes without significant difference between  
201 them (Figs. 2a1, 2a2, 2e). From 21 days onwards, the dimensional increase of the olfactory  
202 organ was due to a massive and statistically significant cell proliferation compared to the  
203 previous stage, but without significant differences between the two sexes (Fig. 2e). At 45 days,  
204 mitosis was still intense, comparable to the previous stage (Fig. 2e); the proliferating cells were  
205 mainly localized in the posterior edge of the lamella (Figs. 2b1, 2c1, 2b2, 2c2). In males at stage  
206 90, upon reaching the sexual maturity, the proliferation decreased and stabilized showing values  
207 comparable to those found in adults. Instead, in females the proliferation continued and  
208 appeared to increase again after the mitotic rate decreased at 90 days of age (Fig. 2e). In adults,

209 PCNA-positive cells were still numerous and also present in all the basal layer of female  
210 olfactory lamella (Fig. 2d1), while in males they were restricted to some clusters in the posterior  
211 region of the lamella (Fig. 2d2). At adult stage, the volume of the olfactory lamella was about  
212 twice larger in females compared to males, in line with the ratio of total body size between  
213 females and males~~the relative proportions of the whole body of the two sexes~~ (Fig. 2f).

214 Anti- $G_{\alpha_{olf}}$  antibody labeled the superficial knobs of ciliated OSNs whose cell bodies were  
215 located in the basal third of the olfactory epithelium and showed faint immunopositivity (Fig.  
216 3a). The optical density of the immunopositive reaction evolved without significant difference  
217 between the two sexes and the various stages considered except for 21 and 45 days, in which  
218 the difference between sexes is significant, with the optical density being higher in males at 21  
219 days and in females at 45 days (Fig. 3b). At 21 days of life, the optical density of males  
220 increased by about 45% compared to the averages measured in previous stages. From 45 days  
221 to adulthood the optical density of males returned to the average level recorded in previous fry  
222 stages. The optical density of females reached its higher value at 45 days, thus later than in  
223 males, then it decreased. However, the statistical analysis did not reveal significant differences  
224 between the various stages, even if both F values for females and males were very close to F  
225 critical values: female  $F_{(P<0.05,5,24)}=2.465$  and male  $F_{(P<0.05,5,24)}=2.610$ ; F critical=2.621.

226 Anti-calretinin immunopositivity was found in mOSNs whose cell bodies were located in the  
227 superficial half of the olfactory epithelium (Fig. 3c). The optical density of the  
228 immunohistochemical reaction showed no significant difference neither between sexes at any  
229 considered stage (Fig. 3d), nor between stages, even if, similarly to what observed for  $G_{\alpha_{olf}}$   
230 immunohistochemistry, both F values for females and males were very close to F critical values:  
231 Female  $F_{(P<0.05,5,24)}=2.610$  and male  $F_{(P<0.05,5,24)}=2.246$ ; F Critical=2.621. Also in this case, the  
232 densities apparently increased in 45-day-old guppies.

233 In addition to mOSNs, anti-calretinin immunohistochemistry also detected a subpopulation of  
234 crypt neurons. The intense staining and the shape permitted their easy identification and  
235 counting: crypt cells had a typical rounded or ellipsoidal cell body placed close to the free  
236 surface of the olfactory epithelium (Figs. 4a, 4b). In the case of crypt cells, the total number of  
237 calretinin-positive cells is also ~~directly~~ presented, as their dynamics are exactly opposite to the  
238 trend of cell density. When considering the total number of calretinin-positive crypt cells, the  
239 value remained low, without significant differences among stages at 7, 14, 21 and 45 days after  
240 birth (Fig. 4c). Only in 90 days old fish, crypt cells were significantly more numerous in males  
241 than in females. Starting from 45 days onwards, there was a statistically significant increase in  
242 the total number of crypt cells compared to previous stages. The total number reached the  
243 highest values in adult males and females (Fig. 4c). When the density of immunopositive crypt  
244 cells was considered (Fig. 4d), the trend of the values obtained in the various stages appeared  
245 reversed compared to the trend of the total number of positive crypt cells. In fact, despite the  
246 moderate increase of the total number of calretinin-positive crypt cells, their density decreased  
247 up to the minimum value in the adult stage. In females, the density at 7 days after birth was  
248 significantly higher than other stages. In the following weeks the values gradually decreased  
249 until they stabilized from 45 days onwards. In males, on the other hand, significant differences  
250 in the density values of crypt cells among different stages were not observed. Significant  
251 differences between the two sexes were present only at 7 days, when the value was higher in  
252 females.

253 Comparing the number of calretinin-positive crypt cells obtained in this work with the total  
254 number of crypt cells, which are S100-positive, taken from our previous work (Bettini et al.,  
255 2009, 2012), we have drawn up Table 1 which shows the percentage ratio between these two  
256 types of crypt cells according to age and sex. The subpopulation of calretinin-positive crypt  
257 cells remains predominant in both sexes up to 3 weeks, with percentages ranging between 70%

258 and 90% (Table 1); from 45 days onwards, the ratio gradually decreases to 15% in females and

259 30% in males.

260

261 **Discussion**

262 The immunohistochemical localization of the selected molecular markers allowed us to follow  
263 the dynamics of the different populations of OSNs during the development of the olfactory  
264 mucosa of *P. reticulata*. From hatching up to the adult stage, the three main types of OSNs  
265 showed different behaviors. In particular, cOSNs and mOSNs showed constant density without  
266 particular differences between the stages. Sex-related differences appeared only for cOSNs at  
267 21 and 45 days. Calretinin-positive crypt cells have decreasing density with age. Differences  
268 between sexes appeared only at 7 days.

269 In a previous work (Bettini et al., 2012), we observed that the dimensional increase of the  
270 olfactory organ of *P. reticulata* did not follow a linear trend: in the first 3 weeks the lamella did  
271 not undergo variations, and only afterwards there was an evident growth, which, after 90 days,  
272 led to a clear volumetric difference between males and females. In the present study, the  
273 analysis of proliferative activity shows an increase in mitotic cell number in both sexes between  
274 21 and 45 days of life. PCNA-positive cells observed in the early stages of development are  
275 exclusively located in the basal layer of the epithelium. Due to their small number, we assume  
276 that they predominantly support normal neuronal turnover. The increase in volume does not  
277 affect the thickness, but the extent of the lamellar surface: from 21 days onwards, the greatest  
278 density of proliferating cells is found in the edges of the olfactory organ, in particular the caudal  
279 one, causing a progressive elongation of the lamella. At 90 days of age, the cell division rate  
280 stabilizes in males, remaining similar at the male adult stage, on the contrary it further increases  
281 in females in the adult stage, as their body growth continues to almost double the size of males.  
282 Mousavi-Sabet et al. (2014) reported numerous morphometric changes during the first 50 days  
283 of guppy development. While the growth in length of the body was quite progressive, allometric  
284 growth pattern of snout length became strongly positive between 15 and 20 days after birth, in  
285 line with what we observed in the olfactory organ. We can make some hypotheses in order to  
286 explain why the dimensional development of the olfactory organ undergoes this variation at



287 that particular stage. In fish, gonad formation begins 2 weeks before birth and their structure is  
288 established at 10-14 days post birth (Koya et al., 2003; Mazzoni et al., 2014). However, sex is  
289 unstable in the first weeks after birth and can be affected by administration of androgens, which  
290 can lead to sex reversal (Ortega-Salas et al., 2013). The formation of secondary sexual traits  
291 (caudal coloration, development of gonopodium in males, etc.), which starts approximately  
292 between 2 and 3 weeks of life, appears to be the first indication of guppy sexual identity (Houde,  
293 1998; Evans et al., 2002; Koya et al., 2003). In fact, gametogenesis continues during the  
294 following weeks and is completed around 90-110 days after birth (Koya et al., 2003), but the  
295 formation of rod-shaped gonopodia with clearly visible apical hoods starts courtship activity in  
296 males, long before they can produce sperm (Houde, 1998; Evans et al., 2002). Since olfaction  
297 is involved in reproduction, the increase in size of the snout (and of the olfactory organ) could  
298 be correlated with the morpho-functional differentiation of the sex. But the absence of  
299 differences between male and female proliferation patterns could lead to another possible  
300 explanation. In accordance with Mousavi-Sabet et al. (2003), the rapid increase in *P. reticulata*  
301 snout elongation after 15 days may be related to changing feeding habit, i.e., foraging from  
302 water column to water surface.

303 Examining in more detail the development of the olfactory epithelium, we observed that the  
304 density of cONSs and mONSs remained constant from the first week of life up to the adult  
305 stage, with distinction between the two sexes only for cOSNs at 21 and 45 days. In the  
306 comparison between the stages, the apparent increase, however statistically not significant,  
307 which is visible for cOSNs between 21 and 45 days, could be a fluctuation simply reflecting  
308 the imbalance in the ratio among cell types caused by the intense proliferation activity. It  
309 appears evident that cOSNs and mOSNs are associated with the uptake of odorants linked to  
310 activities that are functionally independent of sex and stage of development. It is well known  
311 that foraging, social interaction, predator and toxicant avoidance and migration are the main

312 behaviors associated with smell in fish (Nikonov & Caprio, 2001; Bazaes et al., 2013; Olivares  
313 & Schmachtenberg, 2019).

314 Odorants have been indicatively divided in few molecular classes with different biological  
315 functions: amino acids, bile salts, nucleotides, polyamines and pheromones (Nikonov & Caprio,  
316 2001; Sato & Sorensen, 2018). Numerous electrophysiological, behavioral and  
317 immunohistochemical studies, integrated with analysis of the molecular machinery of OSNs  
318 and their projection patterns, made it possible to associate some of those classes of odorants  
319 with each of the cell subtypes and suggest their role in the behavioral response (Bazaes et al.,  
320 2013; Olivares & Schmachtenberg, 2019). Both cOSNs and mOSNs appear to respond to amino  
321 acids in several teleost species (Sato & Suzuki, 2001; Hansen et al., 2003; Schmachtenberg &  
322 Bacigalupo, 2004), but cORNs respond preferentially to bile salts, whereas mOSNs are  
323 stimulated much more by amino acids and also by nucleotides (Hansen et al., 2003; Sato et al.,  
324 2005; Koide et al., 2009; Bazaes et al., 2013; Olivares & Schmachtenberg, 2019). Bile salts,  
325 mainly released into the water through feces and urine, are potential social odorants, that could  
326 play a role in identification of conspecifics, alarm response and territorial demarcation  
327 (Nikonov & Caprio, 2001; Hamdani & Døving, 2007; Bazaes et al., 2013). Nucleotides, instead,  
328 serve as feeding cues (Nikonov & Caprio, 2001; Hansen et al., 2003; Wakisaka et al., 2017;  
329 Sato & Sorensen, 2018). Amino acids are also a well-known category of food odorants (Hansen  
330 et al., 2003; Hara, 2006; Nikonov & Caprio, 2007; Miklavc & Valentinčič, 2012; Sato &  
331 Sorensen, 2018), but they appear to be also involved in behaviors other than feeding, such as  
332 homing (Yamamoto & Ueda, 2009) and reproduction (Yambe et al., 2006). Taken together  
333 these data seem to show that cOSNs are more correlated with social recognition among  
334 conspecifics, while mOSNs are more involved in the search for food, even if Biechl et al. (2016)  
335 showed that food odors stimulated both OSN subtypes, while only a subpopulation of mOSNs  
336 but not cOSNs detected kin odor related signal in zebrafish. These perceptions appear equally

337 important at all stages of development and the constant density of both cell types (cOSNs and  
338 mOSNs) that we observed during guppy development seems to be in accordance. However, at  
339 the moment the meaning of the difference between sexes at 21 and 45 days for cOSNs remains  
340 unclear. This difference could depend on an oscillation, although not significant, of the density  
341 values due to the increased proliferation of basal cells that in males is a few days earlier  
342 compared to females.

343 Interestingly, it has been observed that in the fish *Astyanax mexicanus*, present in two forms  
344 adapted to different environments, the proportions between cOSNs and mOSNs are different  
345 (Blin et al., 2018). cOSNs were more represented in the surface-dwelling form, which is more  
346 oriented towards the sense of sight, while mOSNs were more abundant in the cave-adapted  
347 form, in which the sense of smell has predominant importance, given the reduction/absence of  
348 eyes. In both morphs, the proliferation, cell death, lifespan and neurogenesis patterns in the  
349 developing olfactory epithelium were identical, and very similar also between the two neuron  
350 subtypes, analogously to what we observed in guppies. It could have been interesting to  
351 compare the number of cOSNs and mOSNs in the guppy, but the immunohistochemical  
352 markers, especially the  $G_{\alpha_{olf}}$ , do not allow easy cell counting, so we used an indirect estimate  
353 of densities, which thus cannot be compared. A possible solution to be considered to better  
354 distinguish and quantify the various OSN populations could be the use of transgenic fish, so far  
355 effectively tested by Ma et al. (2018) in zebrafish, but that will be hopefully possible in the  
356 future also for *P. reticulata*.

357 The third population of OSNs, crypt cells, has been associated to pheromone perception and  
358 reproduction in numerous studies (Hamdani & Døving, 2006; Bazáes & Schmachtenberg, 2012;  
359 Ahuja et al., 2013; Bazaes et al., 2013; Olivares & Schmachtenberg, 2019). As further support  
360 for this hypothesis, in *Carassius carassius* (Hamdani et al., 2008) the number of crypt cells  
361 varies throughout the year, increasing during the summer spawning season. Moreover, the

362 differentiation of crypt cells in the olfactory epithelium of the hermaphrodite *Pseudapocryptes*  
363 *lanceolatus* is synchronized with the annual development of ovarian structures in the summer,  
364 and they undergo apoptosis when the breeding season is over (Sarkar & De, 2018). We also  
365 observed that S100-positive crypt cell development correlates with sex and gonadal maturation  
366 in *P. reticulata*, with different dynamics and densities between males and females (Bettini et  
367 al., 2012). However, in another study (Bettini et al., 2017), we observed that crypt cells in *P.*  
368 *reticulata* do not constitute an immunohistochemically uniform population, identifying a  
369 subpopulation of calretinin-positive cells (the population analyzed in the present study). Also,  
370 Parisi et al. (2014) described, in zebrafish, a separate population of calretinin-positive crypt  
371 cells, even if they showed no co-localization of S100 and calretinin proteins. In the present  
372 study, we analyzed how this specific subpopulation of calretinin-positive crypt cells evolves  
373 during the first 6 months of postnatal life. Their number increases in line with epithelial size,  
374 with no substantial differences between males and females, even if in males it seems to start  
375 earlier. The density, however, remains almost constant in males and only slightly decreasing in  
376 females, with divergences between the two sexes at 7 days. Particularly interesting is the  
377 percentage ratio between this calretinin-positive subpopulation and the totality of crypt cells: at  
378 7 days of life, calretinin-positive crypt cells are over 75% in both sexes, but this percentage  
379 gradually decreases after 3 weeks, reaching less than 30% in adult males and even 15% in adult  
380 females. It can be easily assumed that the two subpopulations have different functions:  
381 calretinin-positive cells, similarly to cOSNs and mOSNs, are linked to the perception of odors  
382 important from the first day of life to adulthood, while the other crypt cells become numerically  
383 preponderant only upon reaching sexual maturity, indicating a role connected to reproduction.  
384 Sandulescu et al. (2011) also described an early onset of crypt cell differentiation in zebrafish,  
385 at a stage similar to cOSNs and mOSNs, implying a probable functional significance in first  
386 life stages. It is known that crypt cells can respond to amino acids (Vielma et al., 2008);

387 moreover, in calcium imaging experiments on the rainbow trout (Bazáes & Schmachtenberg,  
388 2012), it was observed that in young fish, crypt cells respond more to amino acids and bile salts,  
389 but in mature fish crypt cells are activated preferentially with exposure to gonadal extracts and  
390 hormones from the opposite sex. The authors suggested that, during development, the crypt cell  
391 population changed sensitivity and function, by replacing common odorant-sensitive cells with  
392 pheromone-sensitive ones. Complementing previous research (Bettini et al., 2012, 2017),  
393 present study appears to support the simultaneous presence of two distinct subpopulations of  
394 crypt neurons, with autonomous functions, modalities and times of development.

### 395 **Conclusions**

396 In this study we analyzed the development of the olfactory organ of *P. reticulata* that does not  
397 show a constant and progressive trend, but has a dimensional increase that begins three weeks  
398 after hatching with a massive proliferative activity. The density of cOSNs and mOSNs remains  
399 stable, with no differences between stages while sex related distinctions appear only for cOSNs  
400 at 21 and 45 days. Calretinin-positive crypt cell density decreases with age despite the  
401 simultaneous increase in the total number of these cells, probably due to a large increase in the  
402 size of the olfactory epithelium. The results suggest the role of cOSNs, mOSNs and calretinin-  
403 positive crypt cells in the uptake of odorants related to basic functions, such as search for food  
404 and social relations. However, many gaps remain in the understanding of the sensory  
405 capabilities of OSN subtypes, also because other factors influence the olfactory perception,  
406 making the data analysis very complex. Many factors appear to influence OSN sensitivity, as  
407 documented for example in zebrafish for the integration between alarm-response behavior and  
408 mating (Diaz-Verdugo et al., 2019), imprinting among siblings (Biechl et al., 2016), and  
409 neuropeptide expression (Kaniganti et al., 2021). Also, environmental changes can alter sensory  
410 capacity by modifying the composition of the epithelium, either for pollutants (Iqbal & Byrd-  
411 Jacobs, 2010; Dew et al., 2012, 2014, 2016; Lazzari et al., 2017, 2019, 2021) or by improving

412 the olfactory detection capacities, without affecting the organ size, as reported in visual-  
413 deprived *Astyanax mexicanus* (Blin et al., 2018).

#### 414 **Financial support**

415 This work was supported by national public funds grant RFO2021FRANCESCHINI from the  
416 Italian Ministry of University and Research (MUR).

417

#### 418 **Conflict of interest**

419 The authors declare that they have no conflicts of interest.

420

421

422 **References**

- 423 Ahuja G, Ivandić I, Saltürk M, Oka Y, Nadler W & Korsching SI (2013). Zebrafish crypt  
424 neurons project to a single, identified mediodorsal glomerulus. *Sci Rep* **3**, 2063.  
425 <https://doi.org/10.1038/srep02063>
- 426 Ahuja G, Nia SB, Zapilko V, Shiriagin V, Kowatschew D, Oka Y & Korsching SI (2014).  
427 Kappe neurons, a novel population of olfactory sensory neurons. *Sci Rep* **4**, 4037.  
428 <https://doi.org/10.1038/srep04037>
- 429 Antunes AM, Rocha TL, Pires FS, de Freitas MA, Milhomem Cruz Leite VR, Arana S, Moreira  
430 PC & Teixeira Saboia-Morais SM (2017). Gender-specific histopathological response in  
431 guppies *Poecilia reticulata* exposed to glyphosate or its metabolite  
432 aminomethylphosphonic acid. *J Appl Toxicol* **37**(9), 1098-1107.  
433 <https://doi.org/10.1002/jat.3461>
- 434 Bazáes A & Schmachtenberg O (2012). Odorant tuning of olfactory crypt cells from juvenile  
435 and adult rainbow trout. *J Exp Biol* **215**(10), 1740-1748.  
436 <https://doi.org/10.1242/jeb.067264>
- 437 Bazáes A, Olivares J & Schmachtenberg O (2013). Properties, projections, and tuning of  
438 teleost olfactory receptor neurons. *J Chem Ecol* **39**(4), 451-464.  
439 <https://doi.org/10.1007/s10886-013-0268-1>
- 440 Bettini S, Ciani F & Franceschini V (2006). Cell proliferation and growth-associated protein  
441 43 expression in the olfactory epithelium in *Poecilia reticulata* after copper solution  
442 exposure. *Eur J Histochem* **50**(2), 141-146.
- 443 Bettini S, Lazzari M, Ciani F & Franceschini V (2009). Immunohistochemical and  
444 histochemical characteristics of the olfactory system of the guppy, *Poecilia reticulata*  
445 (Teleostei, Poeciliidae). *Anat Rec (Hoboken)* **292**(10), 1569-1576.  
446 <https://doi.org/10.1002/ar.20944>

447 Bettini S, Lazzari M & Franceschini V (2012). Quantitative analysis of crypt cell population  
448 during postnatal development of the olfactory organ of the guppy, *Poecilia reticulata*  
449 (Teleostei, Poeciliidae), from birth to sexual maturity. *J Exp Biol* **215**(15), 2711-2715.  
450 <https://doi.org/10.1242/jeb.069039>

451 Bettini S, Lazzari M, Ferrando S, Gallus L & Franceschini V (2016). Histopathological analysis  
452 of the olfactory epithelium of zebrafish (*Danio rerio*) exposed to sublethal doses of urea. *J*  
453 *Anat* **228**(1), 59-69. <https://doi.org/10.1111/joa.12397>

454 Bettini S, Milani L, Lazzari M, Maurizii MG & Franceschini V (2017). Crypt cell markers in  
455 the olfactory organ of *Poecilia reticulata*: analysis and comparison with the fish model  
456 *Danio rerio*. *Brain Struct Funct* **222**(7), 3063-3074. [https://doi.org/10.1007/s00429-017-](https://doi.org/10.1007/s00429-017-1386-2)  
457 [1386-2](https://doi.org/10.1007/s00429-017-1386-2)

458 Biechl D, Tietje K, Gerlach G & Wullimann MF (2016). Crypt cells are involved in kin  
459 recognition in larval zebrafish. *Sci Rep* **6**, 24590. <https://doi.org/10.1038/srep24590>

460 Blin M, Tine E, Meister L, Elipot Y, Bibliowicz J, Espinasa L & Rétaux S (2018).  
461 Developmental evolution and developmental plasticity of the olfactory epithelium and  
462 olfactory skills in Mexican cavefish. *Dev Biol* **441**(2), 242-251.  
463 <https://doi.org/10.1016/j.ydbio.2018.04.019>

464 Braubach OR, Fine A & Croll RP (2012). Distribution and Functional Organization of  
465 Glomeruli in the Olfactory Bulbs of Zebrafish (*Danio rerio*). *J Comp Neurol* **520**(11),  
466 2317-2339. <https://doi.org/10.1002/cne.23075>

467 Dew WA, Wood CM & Pyle GG (2012). Effects of continuous copper exposure and calcium  
468 on the olfactory response of fathead minnows. *Environ Sci Technol* **46**(16), 9019-9026.  
469 <https://doi.org/10.1021/es300670p>



470 Dew WA, Azizishirazi A & Pyle GG (2014). Contaminant-specific targeting of olfactory  
471 sensory neuron classes: connecting neuron class impairment with behavioural deficits.  
472 *Chemosphere* **112**, 519-525. <https://doi.org/10.1016/j.chemosphere.2014.02.047>

473 Dew WA, Veldhoen N, Carew AC, Helbing CC & Pyle GG (2016). Cadmium-induced  
474 olfactory dysfunction in rainbow trout: Effects of binary and quaternary metal mixtures.  
475 *Aquat Toxicol* **172**, 86-94. <https://doi.org/10.1016/j.aquatox.2015.12.018>

476 Diaz-Verdugo C, Sun GJ, Fawcett CH, Zhu P & Fishman MC (2019). Mating suppresses alarm  
477 response in zebrafish. *Curr Biol* **29**(15), 2541-2546.e3.  
478 <https://doi.org/10.1016/j.cub.2019.06.047>

479 Evans JP, Pitcher TE & Magurran AE (2002). The ontogeny of courtship, colour and sperm  
480 production in male guppies. *J Fish Biol* **60**(2), 495-498. [https://doi.org/10.1111/j.1095-](https://doi.org/10.1111/j.1095-8649.2002.tb00299.x)  
481 [8649.2002.tb00299.x](https://doi.org/10.1111/j.1095-8649.2002.tb00299.x)

482 Farbman AI (2000). Cell biology of olfactory epithelium. In The neurobiology of taste and  
483 smell, Finger TE, Silver WL & Restrepo D (Eds.), pp 131-158. New York: Wiley,

484 Ferrando S, Bottaro M, Gallus L, Girosi L, Vacchi M & Tagliafierro G (2006). Observations of  
485 crypt neuron-like cells in the olfactory epithelium of a cartilaginous fish. *Neurosci Lett*  
486 **403**(3), 280-282. <https://doi.org/10.1016/j.neulet.2006.04.056>

487 Ferrando S, Bottaro M, Pedemonte F, De Lorenzo S, Gallus L & Tagliafierro G (2007).  
488 Appearance of crypt neurons in the olfactory epithelium of the skate *Raja clavata* during  
489 development. *Anat Rec (Hoboken)* **290**(10), 1268-1272. <https://doi.org/10.1002/ar.20584>

490 Frontini A, Zaidi AU, Hua H, Wolak TP, Greer CA, Kafitz KW, Li W & Zielinski BS (2003).  
491 Glomerular territories in the olfactory bulb from the larval stage of the sea lamprey  
492 *Petromyzon marinus*. *J Comp Neurol* **465**(1), 27-37. <https://doi.org/10.1002/cne.10811>

493 Gayoso JÁ, Castro A, Anadón R & Manso MJ (2011). Differential bulbar and extra bulbar  
494 projections of diverse olfactory receptor neuron populations in the adult zebrafish (*Danio*  
495 *rerio*). *J Comp Neurol* **519**(2), 247-276. <https://doi.org/10.1002/cne.22518>

496 Gayoso J, Castro A, Anadón R & Manso MJ (2012). Crypt cells of the zebrafish *Danio rerio*  
497 mainly project to the dorsomedial glomerular field of the olfactory bulb. *Chem Senses*  
498 **37**(4), 357-369. <https://doi.org/10.1093/chemse/bjr109>

499 Hamdani EH & Døving KB (2006). Specific projection of the sensory crypt cells in the  
500 olfactory system in crucian carp, *Carassius carassius*. *Chem Senses* **31**(1), 63-67.  
501 <https://doi.org/10.1093/chemse/bjj006>

502 Hamdani EH & Døving KB (2007). The functional organization of the fish olfactory system.  
503 *Prog Neurobiol* **82**(2), 80-86. <https://doi.org/10.1016/j.pneurobio.2007.02.007>

504 Hamdani EH, Lastein S, Gregersen F & Døving KB (2008). Seasonal variations in olfactory  
505 sensory neurons—fish sensitivity to sex pheromones explained? *Chem Senses* **33**(2), 119-  
506 123. <https://doi.org/10.1093/chemse/bjm072>

507 Hansen A & Finger TE (2000). Phyletic distribution of crypt-type olfactory receptor neurons  
508 in fishes. *Brain Behav Evol* **55**(2), 100-110. <https://doi.org/10.1159/000006645>

509 Hansen A & Zeiske E (1998). The peripheral olfactory organ of the zebrafish, *Danio rerio*: an  
510 ultrastructural study. *Chem Senses* **23**(1), 39-48. <https://doi.org/10.1093/chemse/23.1.39>

511 [10.1093/chemse/23.1.39](https://doi.org/10.1093/chemse/23.1.39)

512 Hansen A & Zielinski BS (2005). Diversity in the olfactory epithelium of bony fishes:  
513 development, lamellar arrangement, sensory neuron cell types, and transduction  
514 components. *J Neurocytol* **34**(3-5), 183-208. <https://doi.org/10.1007/s11068-005-8353-1>

515 Hansen A, Eller P, Finger TE & Zeiske E (1997). The crypt cell: a microvillous ciliated  
516 olfactory receptor cell in teleost fishes. Nineteenth annual meeting of the association for  
517 chemoreception sciences (AchemS XIX) and the twelfth international symposium on

518 olfaction and taste (ISOT XII) *Chem Senses* **22**(6), 694-695.  
519 <https://doi.org/10.1093/chemse/22.6.635>

520 Hansen A, Rolen SH, Anderson K, Morita Y, Caprio J & Finger TE (2003). Correlation between  
521 olfactory receptor cell type and function in the channel catfish. *J Neurosci* **23**(28), 9328 -  
522 9339. <https://doi.org/10.1523/JNEUROSCI.23-28-09328.2003>

523 Hansen A, Anderson KT & Finger TE (2004). Differential distribution of olfactory receptor  
524 neurons in goldfish: structural and molecular correlates. *J Comp Neurol* **477**(4), 347-359.  
525 <https://doi.org/10.1002/cne.20202>

526 Hara TJ (2006). Feeding behaviour in some teleosts is triggered by single amino acids primarily  
527 through olfaction. *J Fish Biol* **68**(3), 810-825. <https://doi.org/10.1111/j.0022-1112.2006.00967.x>  
528

529 Houde AE (1998). 2. Reproductive biology and sexual behavior. In *Sex, color, and mate choice*  
530 *in guppies*, Houde AE (Ed.), pp. 29-44. Princeton: Princeton University Press.  
531 <https://doi.org/10.1515/9780691207261-003>

532 Iqbal T & Byrd-Jacobs C (2010). Rapid degeneration and regeneration of the zebrafish  
533 olfactory epithelium after triton X-100 application. *Chem Senses* **35**(5), 351-361.  
534 <https://doi.org/10.1093/chemse/bjq019>

535 Kaniganti T, Deogade A, Maduskar A, Mukherjee A, Guru A, Subhedar N & Ghose A  
536 (2021). Sensitivity of olfactory sensory neurons to food cues is tuned to nutritional states  
537 by Neuropeptide Y signaling. *J Neurochem* **159**(6), 1028-1044.  
538 <https://doi.org/10.1111/jnc.15488>

539 Kinnberg K & Toft G (2003). Effects of estrogenic and antiandrogenic compounds on the testis  
540 structure of the adult guppy (*Poecilia reticulata*). *Ecotoxicol Environ Saf* **54**(1), 16-24.  
541 [https://doi.org/10.1016/s0147-6513\(02\)00010-6](https://doi.org/10.1016/s0147-6513(02)00010-6)

542 Koide T, Miyasaka N, Morimoto K, Asakawa K, Urasaki A, Kawakami K & Yoshihara Y  
543 (2009). Olfactory neural circuitry for attraction to amino acids revealed by transposon  
544 mediated gene trap approach in zebrafish. *Proc Natl Acad Sci USA* **106**(24), 9884-9889.  
545 <https://doi.org/10.1073/pnas.0900470106>

546 Koya Y, Fujita A, Niki F, Ishihara E & Miyama H (2003). Sex differentiation and pubertal  
547 development of gonads in the viviparous mosquitofish, *Gambusia affinis*. *Zoolog Sci*  
548 **20**(10), 1231-1242. <https://doi.org/10.2108/zsj.20.1231>

549 Lazzari M, Bettini S, Ciani F & Franceschini V (2007). Light and transmission electron  
550 microscopy study of the peripheral olfactory organ of the guppy, *Poecilia reticulata*  
551 (Teleostei, Poeciliidae). *Microsc Res Tech* **70**(9), 782-789.  
552 <https://doi.org/10.1002/jemt.20487>

553 Lazzari M, Bettini S & Franceschini V (2013). Immunocytochemical characterization of  
554 olfactory ensheathing cells in fish. *Brain Struct Funct* **218**(2), 539-549.  
555 <https://doi.org/10.1007/s00429-012-0414-5>

556 Lazzari M, Bettini S, Milani L, Maurizii MG & Franceschini V (2017). Differential response  
557 of olfactory sensory neuron populations to copper ion exposure in zebrafish. *Aquatic*  
558 *Toxicol* **183**, 54-62. <https://doi.org/10.1016/j.aquatox.2016.12.012>

559 Lazzari M, Bettini S, Milani L, Maurizii MG & Franceschini V (2019). Differential nickel-  
560 induced responses of olfactory sensory neuron populations in zebrafish. *Aquatic Toxicol*  
561 **206**, 14-23. <https://doi.org/10.1016/j.aquatox.2018.10.011>

562 Lazzari M, Bettini S, Milani L, Maurizii MG & Franceschini V (2021). Response of olfactory  
563 sensory neurons to mercury ions in zebrafish: an immunohistochemical study. *Microsc*  
564 *Microanal* **28**(1), 227-242. <https://doi.org/10.1017/S1431927621013763>

565 Ma EY, Heffern K, Cheres J & Gallagher EP (2018). Differential copper-induced death and  
566 regeneration of olfactory sensory neuron populations and neurobehavioral function in

567 larval zebrafish. *Neurotoxicology* **69**, 141-151.  
568 <https://doi.org/10.1016/j.neuro.2018.10.002>

569 Mazzoni TS, Grier HJ & Quagio-Grassiotto I (2014). Male gonadal differentiation and the  
570 paedomorphic evolution of the testis in teleostei. *Anat Rec* **297**(6), 1137-1162.  
571 <https://doi.org/10.1002/ar.22915>

572 Miklavc P & Valentinčić T (2012). Chemotopy of amino acids on the olfactory bulb predicts  
573 olfactory discrimination capabilities of zebrafish *Danio rerio*. *Chem Senses* **37**(1), 65-75.  
574 <https://doi.org/10.1093/chemse/bjr066>

575 Milani L, Cinelli F, Iannello M, Lazzari M, Franceschini V & Maurizii MG (2022).  
576 Immunolocalization of Vasa, PIWI, and TDRKH proteins in male germ cells during  
577 spermatogenesis of the teleost fish *Poecilia reticulata*. *Acta Histochem* **124**(3), 151870.  
578 <https://doi.org/10.1016/j.acthis.2022.151870>

579 Morita Y & Finger TE (1998). Differential projections of ciliated and microvillous olfactory  
580 receptor cells in the catfish, *Ictalurus punctatus*. *J Comp Neurol* **398**(4), 539-550.  
581 [https://doi.org/10.1002/\(sici\)1096-9861\(19980907\)398:4<539::aid-cne6>3.0.co;2-3](https://doi.org/10.1002/(sici)1096-9861(19980907)398:4<539::aid-cne6>3.0.co;2-3)

582 Mousavi-Sabet H, Azimi H, Eagderi S, Bozorgi S & Mahallatipour B (2014). Growth and  
583 morphological development of guppy *Poecilia reticulata* (Cyprinodontiformes,  
584 Poeciliidae) larvae. *Poec Res* **4**(1), 24-30. [http://www.pr.bioflux.com.ro/docs/2014.24-](http://www.pr.bioflux.com.ro/docs/2014.24-30.pdf)  
585 [30.pdf](http://www.pr.bioflux.com.ro/docs/2014.24-30.pdf)

586 Nikonov AA & Caprio J (2001). Electrophysiological evidence for a chemotopy of biologically  
587 relevant odors in the olfactory bulb of the channel catfish. *J Neurophysiol* **86**(4), 1869-  
588 1876. <https://doi.org/10.1152/jn.2001.86.4.1869>

589 Nikonov AA & Caprio J (2007). Highly specific olfactory receptor neurons for types of amino  
590 acids in the channel catfish. *J Neurophysiol* **98**(4), 1909-1918.  
591 <https://doi.org/10.1152/jn.00548.2007>

592 Olivares J & Schmachtenberg O (2019). An update on anatomy and function of the teleost  
593 olfactory system. *PeerJ* **7**, e7808. <https://doi.org/10.7717/peerj.7808>

594 Ortega-Salas A, Reyes-Bustamante H & Reyes BH (2013). Sex reversal, growth, and survival  
595 in the guppy *Poecilia reticulata* (Cyprinodontiformes: Poeciliidae) under laboratory  
596 conditions. *UNED Res J* **5**(2), 245-248. <https://doi.org/10.22458/urj.v5i2.278>

597 Parisi V, Guerrera MC, Abbate F, Garcia-Suarez O, Viña E, Vega JA & Germanà A (2014).  
598 Immunohistochemical characterization of the crypt neurons in the olfactory epithelium of  
599 adult zebrafish. *Ann Anat* **196**, 178-182. <https://doi.org/10.1016/j.aanat.2014.01.004>

600 Poncelet G & Shimeld SM (2020). The evolutionary origins of the vertebrate olfactory system.  
601 *Open Biol* **10**(12), 200330. <https://doi.org/10.1098/rsob.200330>

602 Riddle DR & Oakley B (1991). Evaluation of projection patterns in the primary olfactory  
603 system of rainbow trout. *J Neurosci* **11**(12), 3752-3762.  
604 <https://doi.org/10.1523/JNEUROSCI.11-12-03752.1991>

605 Sandulescu CM, Teow RY, Hale ME & Zhang C (2011). Onset and dynamic expression of  
606 S100 proteins in the olfactory organ and the lateral line system in zebrafish development.  
607 *Brain Res* **1383**, 120-127. <https://doi.org/10.1016/j.brainres.2011.01.087>

608 Sarkar SK & De SK (2018). Ultrastructure based morphofunctional variation of olfactory crypt  
609 neuron in a monomorphic protogynous hermaphrodite mudskipper (Gobiidae:  
610 Oxudercinae) (*Pseudapocryptes lanceolatus* [Bloch and Schneider]). *J Microsc Ultrastruct*  
611 **6**(2), 99-104. [https://doi.org/10.4103/JMAU.JMAU\\_18\\_18](https://doi.org/10.4103/JMAU.JMAU_18_18)

612 Sato K & Sorensen PW (2018). The chemical sensitivity and electrical activity of individual  
613 olfactory sensory neurons to a range of sex pheromones and food odors in the goldfish.  
614 *Chem Senses* **43**(4), 249-260. <https://doi.org/10.1093/chemse/bjy016>

615 Sato K & Suzuki N (2001). Whole-cell response characteristics of ciliated and microvillous  
616 olfactory receptor neurons to amino acids, pheromone candidates and urine in rainbow  
617 trout. *Chem Senses* **26**(9), 1145-1156. <https://doi.org/10.1093/chemse/26.9.1145>

618 Sato Y, Miyasaka N & Yoshihara Y (2005). Mutually exclusive glomerular innervation by two  
619 distinct transgenic zebrafish. *J Neurosci* **25**(20), 4889-4897.  
620 <https://doi.org/10.1523/JNEUROSCI.0679-05.2005>

621 Schmachtenberg O (2006). Histological and electrophysiological properties of crypt cells from  
622 the olfactory epithelium of the marine teleost *Trachurus symmetricus*. *J Comp Neurol*  
623 **495**(1), 113-121. <https://doi.org/10.1002/cne.20847>

624 Schmachtenberg O & Bacigalupo J (2004). Olfactory transduction in ciliated receptor neurons  
625 of the Cabinza grunt, *Isacia conceptionis* (Teleostei: Haemulidae). *Eur J Neurosci* **20**(12),  
626 3378-3386. <https://doi.org/10.1111/j.1460-9568.2004.03825.x>

627 Souza Trigueiro NS, Gonçalves BB, Cirqueira Diaz F, Celmade Oliveira Lima E, Lopes Rocha  
628 T & Teixeira Saboia-Morais SM (2021). Co-exposure of iron oxide nanoparticles and  
629 glyphosate-based herbicide induces DNA damage and mutagenic effects in the guppy  
630 (*Poecilia reticulata*). *Environ Toxicol Pharmacol* **81**, 103521.  
631 <https://doi.org/10.1016/j.etap.2020.103521>

632 Vielma A, Ardiles A, Delgado L & Schmachtenberg O (2008). The elusive crypt olfactory  
633 receptor neuron: evidence for its stimulation by amino acids and cAMP pathway agonists.  
634 *J Exp Neurol* **211**(15), 2417-2422. <https://doi.org/10.1242/jeb.018796>

635 Wakisaka N, Miyasaka N, Koide T, Masuda M, Hiraki-Kajiyama T & Yoshihara Y (2017). An  
636 adenosine receptor for olfaction in fish. *Curr Biol* **27**(10), 1437-1447.  
637 <https://doi.org/10.1016/j.cub.2017.04.014>

638 Weltzien FA, Hoglund E, Hamdaniel H & Døving KB (2003). Does the lateral bundle of the  
639 medial olfactory tract mediate reproductive behavior in male crucian carp? *Chem Senses*  
640 **28**(4), 293-300. <https://doi.org/10.1093/chemse/28.4.293>

641 Yamamoto M (1982). Comparative morphology of the peripheral olfactory organ in teleosts. In  
642 *Chemoreception in fishes*, Hara TJ (Ed.), pp. 39–59. Amsterdam: Elsevier.

643 Yamamoto Y & Ueda H (2009). Behavioral responses by migratory chum salmon to amino  
644 acids in natal stream water. *Zoolog Sci* **26**(11), 778-782. <https://doi.org/10.2108/zsj.26.778>

645 Yambe H, Kitamura S, Kamio M, Yamada M, Matsunaga S, Fusetani N & Yamazaki F (2006).  
646 L-Kynurenine, an amino acid identified as a sex pheromone in the urine of ovulated female  
647 masu salmon. *Proc Natl Acad Sci USA* **103**(42), 15370-15374.  
648 <https://doi.org/10.1073/pnas.0604340103>

649 Zeiske E, Theisen B & Breucker H (1992). Structure, development and evolutionary aspects of  
650 the peripheral olfactory system. In *Fish Chemoreception*, Hara TJ (Ed.), pp. 13-39.  
651 London: Chapman and Hall.

652



653 **Figure legends**

654 **Fig. 1.** Light microscopic organization of the olfactory organ of adult *Poecilia reticulata*. (a)  
655 In a frontal section of the head, the left olfactory organ appears composed of a single lamella  
656 (arrowheads) protruding into the olfactory cavity. (b) Histological organization of the olfactory  
657 epithelium (E) covering the olfactory lamella. LP, lamina propria. Hematoxylin-eosin. Scale  
658 bars (a), 200  $\mu\text{m}$ ; (b), 20  $\mu\text{m}$ .~~Gonads of 6-month-old *Poecilia reticulata* (Haematoxylin and~~  
659 ~~Eosin). (a) Oocyte, characterized by abundant yolk and large lipid globules, in the adult ovary.~~  
660 ~~(b) Spermatozoa located in groups of spermatozeugmata in the mature cysts of adult testis.~~  
661 ~~Scale bar (1a, 1b), 100  $\mu\text{m}$ .~~

662

663 **Fig. 2.** PCNA immunohistochemistry. **(a1, a2)** Representative micrographs of lamellae with  
664 mitotic cells in the basal layer (arrowheads) in 7-day-old female (a1) and male (a2) guppies.  
665 **(b1, b2)** Representative micrographs of lamellae in 45-day-old female (b1) and male (b2)  
666 guppies: dividing cells are more concentrated in the caudal-posterior region of the olfactory  
667 organ (arrows) than in the basal layer of the central and rostral lamella (arrowhead). **(c1, c2)**  
668 Higher magnification of the caudal region of the olfactory lamella in 45-day-old female (c1)  
669 and male (c2). **(d1, d2)** Representative micrographs of the lamellae in adult female (d1) and  
670 male (d2) guppies: the PCNA-positive cells are mainly located in the caudal-posterior edge of  
671 male olfactory organ (arrow), while in females they are also visible along the basal layer of the  
672 entire lamella (arrowheads). C, caudal; R, rostral; L, lateral; M, medial. Scale bars (a1-b2, d1,  
673 d2), 100  $\mu\text{m}$ ; (c1, c2), 10  $\mu\text{m}$ . **(e)** Density of proliferating cells and statistical comparison among  
674 life stages and between sexes. **(f)** Volume of the olfactory lamella in adult females and males.  
675 Significant differences among stages are indicated by asterisks above the bars, while differences  
676 between sexes for each sampling time are indicated by asterisks superimposed on the bars.

677 Continuous lines, female/female comparison; dotted lines, male/male comparison. \* $P < 0.05$ ,  
678 \*\* $P < 0.01$ ,  $N = 10$ .

679

680 **Fig. 3.**  $G_{\alpha \text{ olf}}$  and calretinin immunohistochemistry. **(a)** Representative micrograph of lamellae  
681 with  $G_{\alpha \text{ olf}}$ -positive cells: immunostaining is mostly visible in the apical knobs of cOSNs  
682 (arrows) but is also present in the cytoplasm of cells throughout the lower half of the epithelium  
683 (arrowheads). Scale bar (a), 20  $\mu\text{m}$ . **(b)** Optical density values of  $G_{\alpha \text{ olf}}$ -positive cOSNs and  
684 statistical comparison among life stages and between sexes. Asterisks indicate significant  
685 male/female differences. \* $P < 0.05$ ,  $N = 10$ . **(c)** Representative micrograph of lamellae with  
686 calretinin-positive cells: they are mOSNs localized in the upper half of the epithelium. Scale  
687 bar (c), 20  $\mu\text{m}$ . **(d)** Optical density values of calretinin-positive mOSNs; there are no significant  
688 differences among stages and between sexes.

689

690 **Fig. 4.** Calretinin-positive crypt cells. **(a, b)** Representative micrographs of stained crypt  
691 neurons with the characteristic ovoid shape (arrows); in some cases, the emerging axon is  
692 clearly visible (arrowhead). Scale bar (a, b): 20  $\mu\text{m}$ . **(c)** Histogram comparing the number of  
693 calretinin-positive crypt cells per animal at various life stages. **(d)** Histogram comparing the  
694 density of calretinin-positive crypt cells at various life stages. Significant differences among  
695 stages are indicated by asterisks above the bars, while differences between sexes for each  
696 sampling time are indicated by asterisks superimposed on the bars. Continuous lines,  
697 female/female comparison; dotted lines, male/male comparison. \* $P < 0.05$ , \*\* $P < 0.01$ ,  $N = 10$ .

698

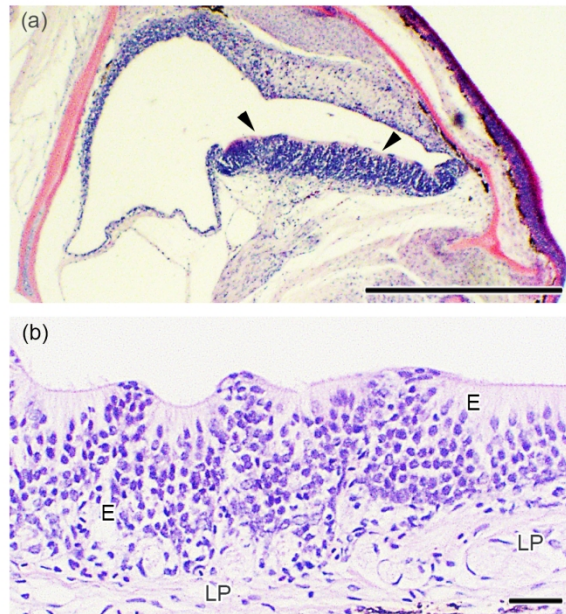


Fig. 1. Light microscopic organization of the olfactory organ of *Poecilia reticulata*  
161x108mm (300 x 300 DPI)

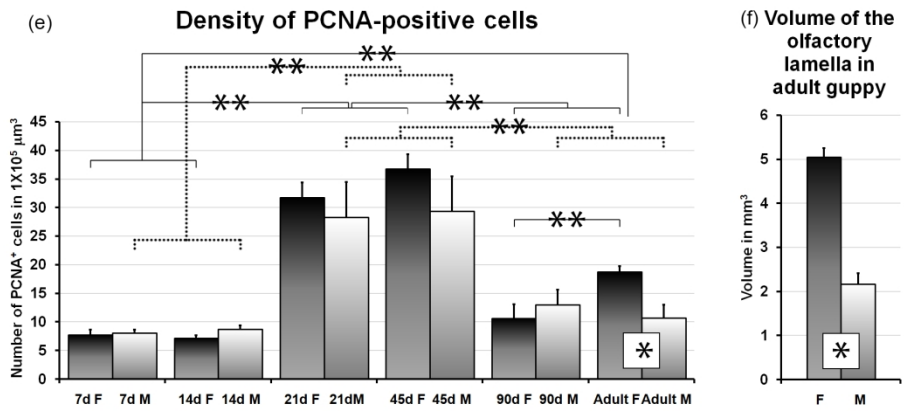
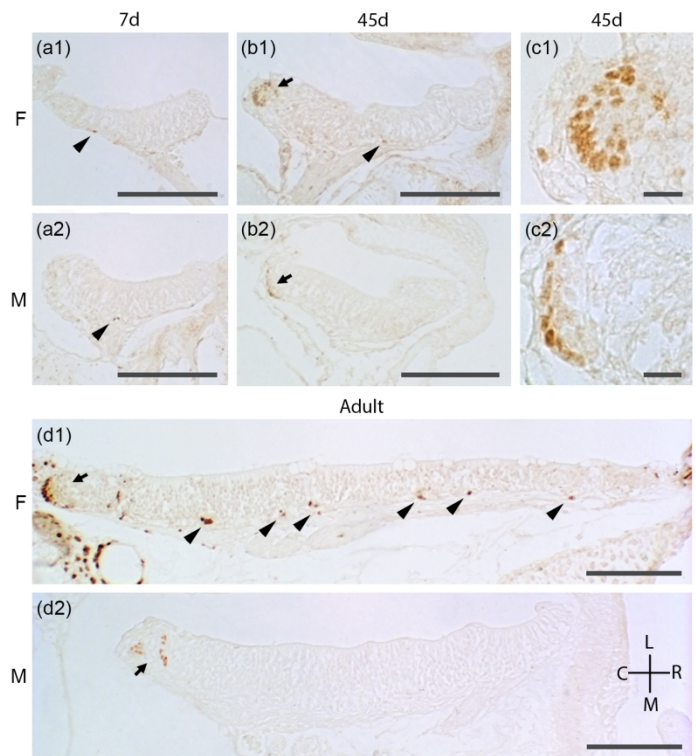


Fig. 2. PCNA immunohistochemistry  
162x216mm (300 x 300 DPI)

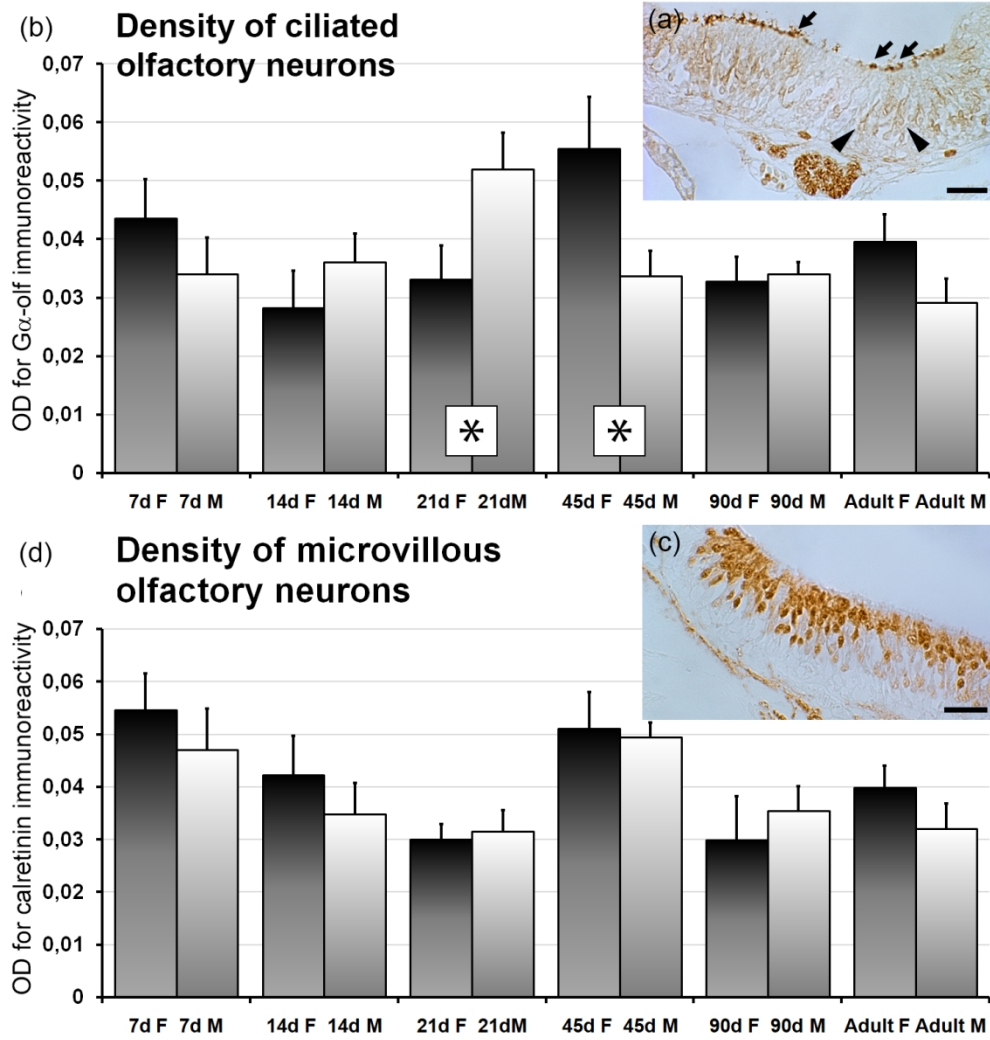


Fig. 3. G $\alpha_{olf}$  and calretinin immunohistochemistry.

127x133mm (300 x 300 DPI)

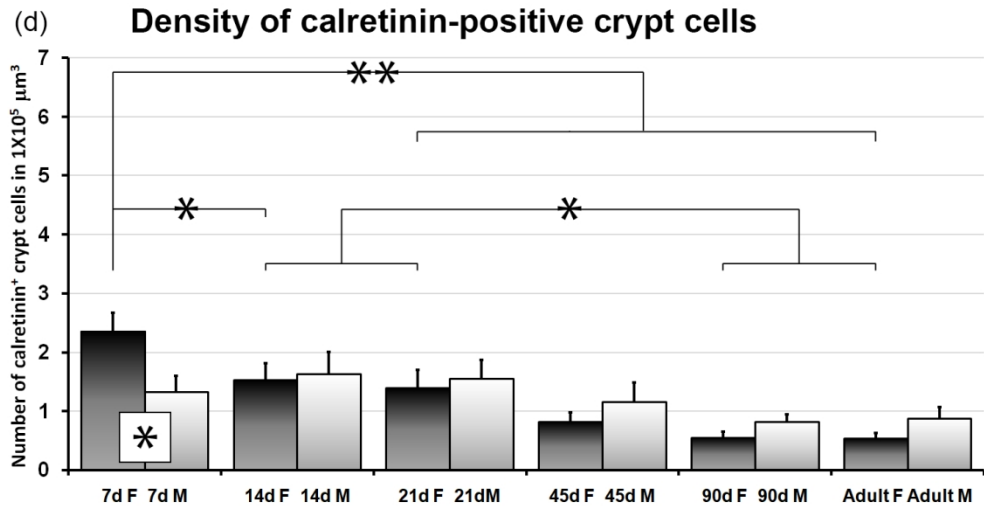
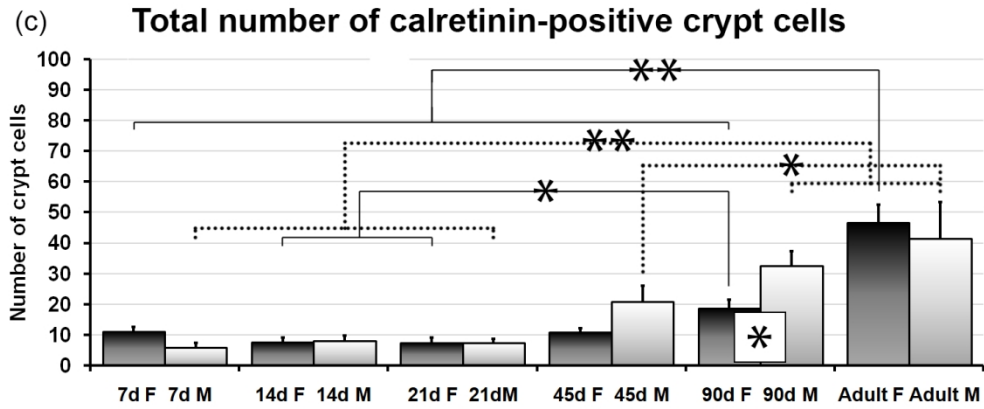
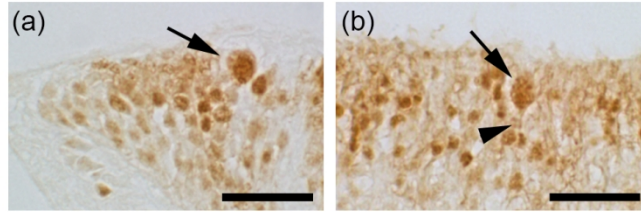


Fig. 4. Calretinin-positive crypt cells.

127x151mm (300 x 300 DPI)

**Table 1.** Number of calretinin-positive crypt cells, total number of crypt cells (S100-positive)\*, and their percentage ratio according to age and sex.

FEMALE	Calretinin <sup>+</sup> crypt cells	Total number of crypt cells (S100 <sup>+</sup> )	Calretinin <sup>+</sup> crypt cells S100 <sup>+</sup> crypt cells %
7d	10.8±1.3	13.8±1.4	77.93%
14d	7.7±1.3	9.2±1.7	84.28%
21d	7.4±1.8	8.4±1.3	88.02%
45d	10.9±1.3	27±3	40.62%
90d	19±3	77±6	24.36%
Adult	47±6	297±30	15.74%

MALE	Calretinin <sup>+</sup> crypt cells	Total number of crypt cells (S100 <sup>+</sup> )	Calretinin <sup>+</sup> crypt cells S100 <sup>+</sup> crypt cells %
7d	5.97±1.5	8.5±1.5	70.65%
14d	7.98±1.8	8.7±0.8	91.4%
21d	7.48±1.3	9.9±0.9	75.4%
45d	21±5	28±2	74.81%
90d	33±5	61±5	53.81%
Adult	42±12	139±12	29.82%

Values are mean per animal ± s.e.m.

\* Values taken from Bettini et al., 2009, 2012